Astron. Astrophys. 362, 1151–1157 (2000)

ASTRONOMY AND ASTROPHYSICS

Slow magnetoacoustic waves in coronal loops

V.M. Nakariakov[1], **E. Verwichte**[2], **D. Berghmans**[2], **and E. Robbrecht**[2,3]

[1] Physics Department, University of Warwick, Coventry CV4 7AL, UK (valery@astro.warwick.ac.uk)
[2] Royal Observatory of Belgium, Ringlaan 3, 1180 Brussels, Belgium (Erwin.Verwichte@ksb-orb.oma.be)
[3] Centre for Plasma Astrophysics, K. U. Leuven, Celestijnenlaan 200B, 3001 Heverlee, Belgium

Received 29 June 2000 / Accepted 31 August 2000

Abstract. A theoretical model interpreting propagating disturbances of EUV emission intensity, recently observed in coronal loops, is constructed in terms of slow magnetoacoustic waves. The model is one-dimensional and incorporates effects of nonlinearity, dissipation due to finite viscosity and thermal conduction, and gravitational stratification of plasma in the loop. It has been found that, for the observationally detected parameters of the waves, the main factors influencing the wave evolution are dissipation and stratification. The upwardly propagating waves of observed periods (5–20 min) are found to decay significantly in the vicinity of the loop apex, explaining the rarity of observational detection of downwardly propagating waves. The model provides a theoretical basis for development of MHD seismology of the coronal loops.

Key words: Magnetohydrodynamics (MHD) – waves – Sun: activity – Sun: corona – Sun: oscillations – Sun: UV radiation

1. Introduction

Magnetohydrodynamic waves are believed to play a very important role in the solar corona. In particular, the waves have been theoretically discussed for a couple of decades as a possible source for heating of the coronal plasma and acceleration of the solar wind. However, the main difficulty with testing of the theories has been connected with the lack of observational knowledge on the coronal wave activity. Before SOHO and TRACE, apart from the confident registration of oscillations in prominences (Oliver 1999), main information on coronal oscillations came from the radio band (e.g. see Aschwanden 1987 for a review) and there had only been a few observational reports of waves or oscillations of coronal structures: in coronal green line (Koutchmy et al. 1983), EUV (e.g. Chapman et al. 1972, Antonucci et al. 1984) and soft X-rays (Harrison 1987).

Only with SOHO/EIT and TRACE imaging telescopes, the direct detailed observation and investigation of coronal waves have become possible. Indeed, for the last few years, several types of coronal waves have been discovered. In particular, Thompson et al. (1999) have detected and investigated a global coronal wave generated by the coronal mass ejection or a flare and occupying a significant part of the solar disk. This wave has been called a coronal Moreton wave or EIT wave. This wave is propagating transversely to coronal structures, and is therefore most likely a fast magnetoacoustic wave. The coronal Moreton waves can interact with various coronal structures, generating secondary oscillations and waves in these structures, such as kink oscillations of coronal loops, detected with TRACE (Aschwanden et al. 1999a, Nakariakov et al. 1999).

Analyzing temporal and spatial variation of the emission intensity with SOHO/EIT, DeForest & Gurman (1998) have detected and investigated propagating disturbances of intensity emission at the 171 Å line, in polar plumes. These waves are observed at the distance of 1.01–1.2 $R_\odot$ out of the limb. The quasi-periodic (with periods of about 10–15 min) groups of 3–10 periods, with the roughly balanced duty cycle are propagating outwardly with the speeds of about 75–150 km/s. The amplitude of the intensity perturbations is about 2% of the background. The ratio of the wave amplitude (in intensity) to the background value grows with height (Ofman et al. 1999). These propagating disturbances are probably connected with the periodic density fluctuations (periods $\approx$ 9 min), detected in coronal holes at $1.9R_\odot$ by Ofman et al. (1997, 1998, 2000) using white light channel of the SOHO/UVCS.

Taking into account these observational findings, the propagating compressive disturbances have been confidently interpreted as slow magnetoacoustic waves (Ofman, Nakariakov & Deforst 1999; Ofman, Nakariakov & Sehgal 2000). It has been understood that the main factors affecting the wave evolution are (a) gravitational stratification, leading to amplification of the relative amplitude of the wave, (b) dissipation, extracting the wave energy in the high wave number domain of the spectrum, and (c) nonlinearity, generating higher harmonics and responsible for the wave steepening and consequent enhanced dissipation. An evolutionary equation of the Burgers type, combining action of all of these three mechanisms, has been derived. Also, full MHD nonlinear numerical simulations of the slow wave dynamics have been undertaken. A perfect agreement of the numerical and analytical results, and a good qualitative agreement of the theoretical studies and observational finding have been found.

Investigating dynamics of on-disc coronal active regions, Berghmans & Clette (1999) and Robbrecht et al. (1999), using

Send offprint requests to: V.M. Nakariakov

SOHO/EIT, have detected compressive disturbances propagating along coronal loops. This discovery has been confirmed by Berghmans et al. (1999) and De Moortel et al. (2000) with TRACE. The results turned out to be very similar to the polar plume waves discussed above. Here, there is a brief summary of the observational findings:

1. Perturbations of the intensity (plasma density), propagating *upwardly* along long coronal loops have been detected at the EIT 195 Å (Berghmans & Clette 1999) and TRACE 171 Å (Berghmans et al. 1999, De Moortel et al. 2000) bandpasses.
2. The projections of the propagation speeds are about 65–165 km s^{-1} (Berghmans & Clette 1999), or $> 70 \pm 16$ km s^{-1} (De Moortel et al. 2000).
3. Amplitude is $\approx$ 2–4% in intensity ($\approx$ 1–2% in density) in both 171 Å and 195 Å bandpasses.
4. The periods are about 180–420 s (De Moortel et al. 2000). The periods are well below the acoustic cut-off period, which is about 87 min.
5. The disturbances often show an exponential decay with the decay time of the order of 1.5–2 min (Robbrecht et al. 1999).

According to reports of both these groups, in most cases, only upwardly (from loop footpoints to loop apexes) propagating disturbances have been detected. A multi-wavelength analysis of the propagating disturbances observed simultaneously with EIT and TRACE has recently been undertaken by Robbrecht et al. (2000) and has strengthen the previous findings.

The obvious similarity of compressive propagating disturbances observed in coronal loops and in polar plumes, suggests that, as well as in the plume case, the perturbations of the loops are *slow magnetoacoustic waves*. To support this interpretation, it is necessary to develop a theoretical model for slow magnetoacoustic waves propagating along long loops, similar to the theory of slow waves in plumes developed by Ofman, Nakariakov & Deforest (1999) and Ofman, Nakariakov & Sehgal 2000). The difference in the geometry of the magnetic structures supporting the waves, (in the plume case, it is a radially divergent magnetic flux tube, which cannot be used to model a loop), requires a creation of theory for slow waves in coronal loops. This theory has to incorporate effects of the gravitational stratification, nonlinearity, dissipation and loop curvature. The theory has to explain the observed facts of the evolution of the compressive waves in loops. In particular, the theory has to provide us with an answer to why only the upwardly propagating waves are seen in most cases.

The paper is organized as follows: the model analyzed and governing equations applied are discussed in Sect. 2, an evolutionary equation is derived in Sect. 3 and analyzed in Sect. 4. The summary of results obtained and comparison of the theoretical results with observational findings is presented in Conclusions.

2. The model and governing equations

As a first step, we consider a semi-circular loop of constant cross-section with the curvature radius R_L. The loop is filled with a magnetized isothermal plasma. In our model, we restrict our attention to strictly longitudinal, with respect to the magnetic field, perturbations. In the following, we neglect 2D effects such as the loop curvature and twisting, and transversal structuring. Consequently, we can consider the loop as a straight cylinder, confined between two planes representing the footpoints. The geometry of the problem is shown in Fig. 1.

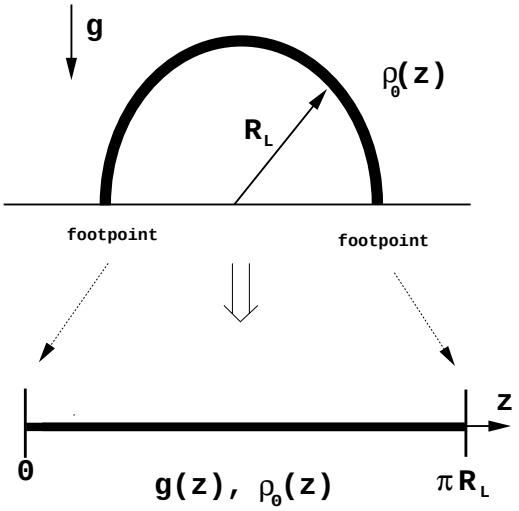

Fig. 1. The sketch of the model considered. A coronal loop is considered as a straight magnetic field line with density and gravitational acceleration varying along the axis of the cylinder.

The plasma β is supposed to be much smaller than unity. As we consider purely parallelly propagating waves, there are two magnetohydrodynamic wave modes in the model, Alfvén waves propagating with the Alfvén speed C_A, and slow magnetoacoustic waves degenerated to the pure acoustic waves, with the sound speed C_s. The Alfvén waves have to be excluded from the consideration, because (a) their speed in the corona is much higher than the observed speed of the running disturbances and (b) the waves are almost incompressible and are not able to create the emission intensity perturbations observed. On the other hand, the slow magnetoacoustic waves are the primary candidates for the interpretation, because they do perturb the plasma density, creating the emission intensity variations and their speed is about the observed propagation speed.

We consider a slow wave propagating strictly along the magnetic field, in the z-direction. The plasma motions are described by the equations

$$\frac{\partial \rho}{\partial t} + \frac{\partial}{\partial z}\left(\rho V\right) = 0, \tag{1}$$

$$\rho\left(\frac{\partial V}{\partial t} + V\frac{\partial V}{\partial z}\right) + \frac{\partial p}{\partial z} + g\rho = \frac{4}{3}\eta_0 \frac{\partial^2 V}{\partial z^2}, \tag{2}$$

$$\frac{dp}{dt} - \frac{\gamma p}{\rho}\frac{d\rho}{dt} = (\gamma - 1)\frac{\partial}{\partial z}\left(\kappa_{||}\frac{\partial T}{\partial z}\right), \tag{3}$$

where ρ is the plasma density, V is the longitudinal speed, p is the plasma pressure, T is plasma temperature, γ is the adiabatic index, $\kappa_{||}$ is thermal conductivity along the magnetic field, η_0 is

the compressive viscosity coefficient, g is the projection of the gravitational acceleration on the z-axis,

$$g = \frac{GM_\odot}{R_\odot^2}\left(1+\frac{R_L}{R_\odot}\sin\frac{z}{R_L}\right)^{-2}\cos\frac{z}{R_L}, \quad (4)$$

with G is the gravitational constant, R_L is the loop radius and $R_\odot$ and $M_\odot$ are solar radius and mass, respectively. In Eq. (3) we neglect radiative losses and heating terms. Connection of T with ρ and p can be obtained from the ideal gas law,

$$T = \frac{p}{\mathcal{R}\rho}, \quad (5)$$

where $\mathcal{R}$ is the gas constant.

The magnetic field guides the waves, but is not explicitly presented in the governing equations. This is because we consider strictly longitudinal waves only. The waves do not perturb the field and their speed is independent of the field strength. Consequently, the magnetic field is absent from the governing equations of our model.

The stationary density ρ_0 and pressure p_0 are connected with each other by relations

$$\frac{dp_0}{dz} = -g\rho_0, \quad (6)$$

which follows from Eq. (1) and the state equation

$$p_0 = \left(C_s^2/\gamma\right)\ \rho_0. \quad (7)$$

We restrict our attention to consideration of the isothermal loops with the stationary temperature $T_0 = \mathrm{const}$, giving $C_s = \mathrm{const}$. The density profile along the loop, following from (4), (6) and (7) is

$$\begin{aligned}\rho_0(z) &= \rho_0(0)\exp\left(-\frac{\gamma}{C_s^2}\int_0^z g(z')\,\mathrm{d}z'\right) \quad (8)\\ &= \rho_0(0)\exp\left(-\frac{\gamma g(0)}{C_s^2}\frac{R_L\sin(z/R_L)}{1+(R_L/R_\odot)\sin(z/R_L)}\right).\end{aligned}$$

3. The evolutionary equation for slow waves

For the following analysis we assume that the effects of nonlinearity and dissipation are both weak. Weakly nonlinear and weakly dissipative perturbations of the stationary state are described by the equations

$$\frac{\partial\rho}{\partial t}+\frac{\partial}{\partial z}\left(\rho_0 V\right) = N_1, \quad (9)$$

$$\rho_0\frac{\partial V}{\partial t}+\frac{\partial p}{\partial z}+g\rho = N_2, \quad (10)$$

$$\frac{\partial p}{\partial t}-C_s^2\frac{\partial\rho}{\partial t}-\frac{C_s^2(\gamma-1)}{\gamma}\frac{\mathrm{d}\rho_0}{\mathrm{d}z}V = N_3, \quad (11)$$

where p, ρ and V are perturbations of pressure, density and velocity. Nonlinear and dissipative terms are gathered on the right handsides of the equations,

$$N_1 = -\frac{\partial}{\partial z}\left(\rho V\right), \quad (12)$$

$$N_2 = -\rho\frac{\partial V}{\partial t}-\rho_0 V\frac{\partial V}{\partial z}+\frac{4}{3}\eta_0\frac{\partial^2 V}{\partial z^2}, \quad (13)$$

$$N_3 = -V\frac{\partial p}{\partial z}+C_s^2\left[\left(\frac{p}{p_0}-\frac{\rho}{\rho_0}\right)\frac{\partial\rho}{\partial t}+V\frac{\partial\rho}{\partial z}\right] + (\gamma-1)\kappa_{||}\frac{\partial^2 T}{\partial z^2}. \quad (14)$$

Eq. (5) provides us with the linear expression for perturbations of the temperature:

$$T = \frac{1}{\mathcal{R}\rho_0}\left(p-\frac{p_0}{\rho_0}\rho\right). \quad (15)$$

In Eq. (3) and consequent Eqs. (11) and (14), we took into account that the background temperature assumed to be constant and, therefore, the thermal conductivity $\kappa_{||}(\propto T_0^{5/2})$ is independent of the coordinate z. Additional terms, connected with the modification of $\kappa_{||}$ by *perturbations* of the temperature, are of higher orders as the thermal conductivity itself is assumed to be small. Consequently, the modification of the thermal conduction by the temperature perturbations is negligible.

Eqs. (9)–(11) can be combined into the wave equation

$$\begin{aligned}&\frac{\partial^2 V}{\partial t^2}-\frac{C_s^2}{\rho_0}\frac{\partial^2}{\partial z^2}\left(\rho_0 V\right)+\frac{C_s^2(\gamma-1)}{\gamma\rho_0}\frac{\partial}{\partial z}\left(\frac{\mathrm{d}\rho_0}{\mathrm{d}z}V\right)\\ &-\frac{g}{\rho_0}\frac{\partial}{\partial z}\left(\rho_0 V\right)\\ &\quad=\frac{1}{\rho_0}\left[\frac{\partial N_2}{\partial t}-\frac{\partial}{\partial z}\left(C_s^2 N_1+N_3\right)-gN_1\right]. \quad (16)\end{aligned}$$

According to (8),

$$\frac{\mathrm{d}\rho_0}{\mathrm{d}z} = -\frac{1}{H}\rho_0, \quad (17)$$

where $H = C_s^2(\gamma g)^{-1}$ is the local density scale height, and

$$\frac{\mathrm{d}^2\rho_0}{\mathrm{d}z^2} = \frac{\rho_0}{H}\left(\frac{1}{H}-\frac{1}{g}\frac{\mathrm{d}g}{\mathrm{d}z}\right). \quad (18)$$

Using expressions (17) and (18), Eq. (16) can be re-written as

$$\begin{aligned}&\frac{\partial^2 V}{\partial t^2}-C_s^2\frac{\partial^2 V}{\partial z^2}+\gamma g\frac{\partial V}{\partial z}+\frac{\mathrm{d}g}{\mathrm{d}z}V =\\ &\frac{1}{\rho_0}\left[\frac{\partial N_2}{\partial t}-\frac{\partial}{\partial z}\left(C_s^2 N_1+N_3\right)-gN_1\right]. \quad (19)\end{aligned}$$

Wave equation (19) describes two slow magnetoacoustic waves propagating in opposite directions. If the nonlinear and dissipative terms on the right handside of (19) and the "inhomogeneous", two last terms on the left handside are all zero, the waves propagating in the opposite directions are decoupled with each other. We restrict our attention to one of the waves, which propagates in the positive direction of z. In the absence of the nonlinearity, dissipation and inhomogeneity, the wave propagates with a constant amplitude and shape in the running frame of reference. The inhomogeneity, dissipation and nonlinearity affect the wave parameters leading to evolution of the

wave. We assume that effects of inhomogeneity, dissipation and nonlinearity are weak. These assumptions are expressed by the non-equalities,

$$\frac{\lambda}{R_L} \ll 1, \quad \frac{\lambda}{H} \ll 1, \quad \frac{\eta_0}{C_s \lambda \rho_0} \ll 1,$$

$$\frac{\kappa_{||}}{C_s \lambda \rho_0 \mathcal{R}} \ll 1, \text{ and } \frac{\rho}{\rho_0} \ll 1, \tag{20}$$

where λ is the wavelength, $H = C_s^2(\gamma g)^{-1}$ is the density scale height and ρ is the density perturbation. The last inequality can also be represented as $V/C_s \ll 1$. Inequalities (20) are supposed to be fulfilled at any time and in any point of the domain considered.

The fourth term on the lefthand side of (19) reaches a maximal value near the footpoints $z = 0,\ \pi R_L$, and decreases to zero near the loop apex. We observe that the ratio of the fourth term to the third term is about λ/R_L and, according to the first inequality from (20), the fourth term can be neglected with respect to the third term.

Under assumptions (20), the wave evolution is slow (with respect to the wave period), which allows us to apply the method of slowly varying amplitude. We change the independent variables

$$\xi = z - C_s t, \quad Z = \epsilon z, \tag{21}$$

where ϵ is a small parameter of order of the inhomogeneity, dissipation and nonlinearity. Note, that the three factors of evolution are not necessary to be of the same order, but each of them is *at least* of order of ϵ less than the first two terms on the lefthand side of Eq. (19) (the "wave" terms).

In the running frame of reference (21), Eq. (19) is re-written as

$$\frac{\partial^2 V}{\partial Z \partial \xi} - \frac{1}{2H}\frac{\partial}{\partial \xi} V =$$

$$- \frac{1}{2C_s^2 \rho_0}\left[C_s \frac{\partial N_2}{\partial \xi} + \frac{\partial}{\partial \xi}\left(C_s^2 N_1 + N_3\right) + g N_1\right], \tag{22}$$

with

$$N_1 = -\frac{\rho_0}{C_s}\frac{\partial V^2}{\partial \xi}, \tag{23}$$

$$N_2 = \frac{4\eta_0}{3}\frac{\partial^2 V}{\partial \xi^2}, \tag{24}$$

$$N_3 = -C_s(\gamma - 1)\rho_0 V \frac{\partial V}{\partial \xi} + \frac{C_s(\gamma-1)^2 \kappa_{||}}{\gamma R}\frac{\partial^2 V}{\partial \xi^2}. \tag{25}$$

Perturbations of other physical values, expressed through V,

$$\rho = \frac{\rho_0}{C_s} V, \quad p = C_s \rho_0 V, \quad T = \frac{C_s(\gamma-1)}{\gamma \mathcal{R}} V, \tag{26}$$

were used in the derivation of Eqs. (22)–(25). Note that only linear expressions were applied, because we restrict our attention to quadratically nonlinear processes.

Taking that, according to (20), H and ρ_0 are functions of the "slow" coordinate Z and integrating Eq. (22) with respect to ξ, we obtain the evolutionary equation for the density perturbations

$$\frac{\partial V}{\partial Z} - \frac{1}{2H} V + \frac{\gamma+1}{2C_s} V \frac{\partial V}{\partial \xi}$$

$$- \frac{1}{2\rho_0 C_s}\left[\frac{4\eta_0}{3} + \frac{\kappa_{||}(\gamma-1)^2}{\gamma \mathcal{R}}\right]\frac{\partial^2 V}{\partial \xi^2} = 0. \tag{27}$$

Eq. (27) is the modified Burgers equation, which takes into account nonlinearity, viscosity and thermal conductivity, stratification and structuring of the plasma.

It is convenient to use the normalized variables $Z = R_\odot Z'$, $\xi = R_\odot \xi'$, $H = R_\odot H'$, $V = C_s V'$ and $\rho_0 = \rho_0(0)\rho_0'$. In the normalized variables, Eq. (27) is re-written as

$$\frac{\partial V'}{\partial Z'} - \frac{1}{2H'} V' + \frac{\gamma+1}{2} V' \frac{\partial V'}{\partial \xi'} - \frac{\bar{\eta}}{2\rho_0'}\frac{\partial^2 V'}{\partial \xi'^2} = 0, \tag{28}$$

where

$$\bar{\eta} = \frac{1}{\rho_0(0) C_s R_\odot}\left[\frac{4\eta}{3} + \frac{\kappa_{||}(\gamma-1)^2}{\mathcal{R}\gamma}\right], \tag{29}$$

is the normalized dissipation coefficient,

$$H' = H(0)\frac{\left[1 + \bar{R}_L \sin(Z/\bar{R}_L)\right]^2}{\cos(Z/\bar{R}_L)}, \tag{30}$$

where $H(0) = C_s^2[\gamma g(0) R_\odot]^{-1}$, and

$$\rho_0' = \exp\left\{-\frac{\bar{R}_L}{H(0)}\frac{\sin(Z/\bar{R}_L)}{1 + \bar{R}_L \sin(Z/\bar{R}_L)}\right\} \tag{31}$$

and $\bar{R}_L = R_L/R_\odot$.

Solutions of Eq. (28) allows us to determine behaviour of other physical values, using expressions (26). The relative perturbations of density, pressure and temperature show the same behaviour as V, but with the different coefficients of proportionality.

$$\frac{\rho}{\rho_0} = \frac{V}{C_s}, \quad \frac{p}{p_0} = \gamma\frac{V}{C_s}, \quad \text{and} \quad \frac{T}{T_0} = (\gamma-1)\frac{V}{C_s}. \tag{32}$$

4. Slow wave evolution

In the case of linear waves and a dissipation-less medium, the third and fourth terms in Eq. (28) are neglected, and the equation is easily integrated:

$$V'(Z') = V'(0)\exp\left[\frac{\bar{R}_L}{2H'(0)}\frac{\sin(Z'/\bar{R}_L)}{1 + \bar{R}_L \sin(Z'/\bar{R}_L)}\right]. \tag{33}$$

The solution is shown as the solid curve in Fig. 2. The amplitude grows until the wave reaches the loop apex and then decays. The amplitude is represented by a symmetric function of Z' with respect to the apex $Z' = \pi\bar{R}_L/2$.

When the dissipation is not zero, but the wave is still linear, a solution of Eq. (28) can be found for a harmonic wave $V' \propto \cos\, k\xi'$ (where k is the wave number):

$$V'(Z') = V'(0)\exp\left[\int_0^{Z'}\left(\frac{1}{2H'(x)} - \frac{k^2\bar{\eta}}{2\rho_0'(x)}\right)\mathrm{d}x\right]. \tag{34}$$

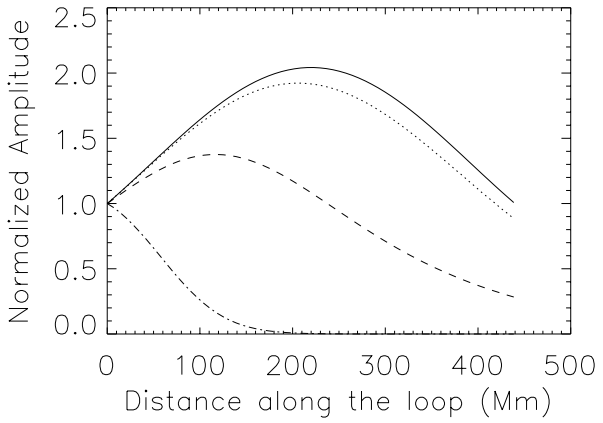

Fig. 2. Evolution of amplitude of slow magnetoacoustic waves propagating along a coronal loop of the radius 140 Mm. The amplitude is measured in units of the initial amplitude $V(0) = 10^{-9}C_s$ and the wave period is 600 s. The solid curve corresponds to the normalized dissipation coefficient $\bar{\eta} = 10^{-9}$, the dotted curve to $\bar{\eta} = 10^{-4}$, the dashed curve to $\bar{\eta} = 10^{-3}$ and the dash-dotted line to $\bar{\eta} = 10^{-2}$. Similar behaviour is shown by relative perturbations of density, pressure and temperature.

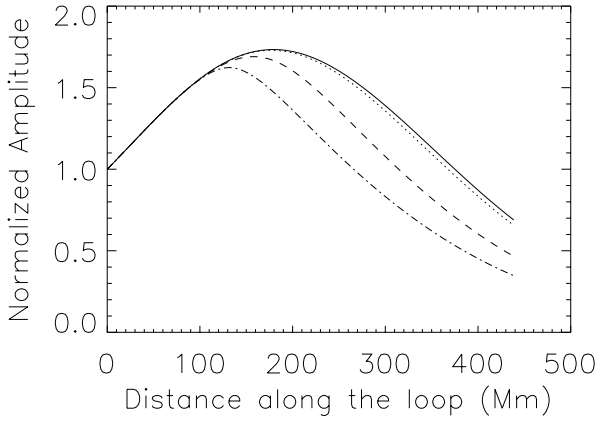

Fig. 3. Evolution of amplitude of slow magnetoacoustic waves with the period 600 s, propagating along a coronal loop of the radius 140 Mm. The normalized dissipation coefficient is $\bar{\eta} = 3 \times 10^{-4}$. The solid curve corresponds to the initial amplitude $V(0) = 0.001C_s$, the dotted curve to $V(0) = 0.03C_s$, the dashed curve to $V(0) = 0.08C_s$ and the dash-dotted line to $V(0) = 0.12C_s$. The amplitude of each wave is measured in units of the initial amplitudes.

According to (30) and (31), the initial stage of the wave evolution, in the vicinity of the footpoint $Z' = 0$, is described by the expression

$$V'(Z') \approx V'(0)\left[1 + \frac{1}{2}\left(\frac{1}{H'(0)} - k^2\bar{\eta}\right) Z'\right]. \qquad (35)$$

Consequently, the growth rate of the amplitude is determined by the balance between the stratification and the dissipation. Waves of shorter wavelengths (larger wavenumbers) grow slower than long wavelength waves. Sufficiently short wavelength waves, with $k > 1/\sqrt{\bar{\eta}H'(0)}$, do not grow but decay with height. Dependences of the linear wave amplitude on the distance along the loop for different values of the normalized dissipation coefficient $\bar{\eta}$ are shown in Fig. 2. Obviously, the dissipative waves are not represented by symmetric curves along the loop. Waves, descending from the loop apex have smaller amplitude than ascending waves.

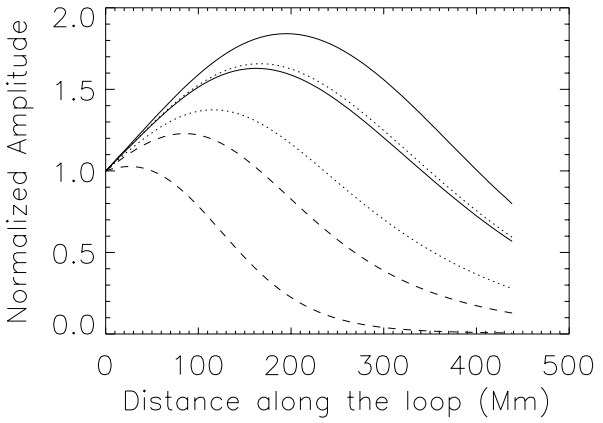

Fig. 4. Evolution of amplitude of slow magnetoacoustic waves with the initial amplitude $V(0) = 0.02C_s$ for three wave periods: 900 s (the solid curves), 600 s (the dotted curves) and 300 s (the dashed curves). The upper curve of each kind corresponds to the normalized dissipation coefficient $\bar{\eta} = 4 \times 10^{-4}$, and the lower curve to $\bar{\eta} = 1 \times 10^{-3}$. The amplitude of each wave is measured in units of the initial amplitude. Other parameters are as in Figs. 2 and 3.

In general, when all terms of Eq. (28) are significant, it is difficult to find out an analytical solution to the equation. However, the equation can be easily solved numerically. Dependence of nonlinear dissipative wave amplitudes on the distance along the loop is shown in Fig. 3. Nonlinear generation of higher harmonics transfers the wave energy to smaller scales, which are, according to subject to stronger dissipation. The nonlinear dissipation increases with the growth of the amplitude. Waves of stronger amplitudes are more non-symmetric with respect to the loop apex.

According to the theory presented above, the slow wave evolution is controlled by the wave parameters: the period and the relative amplitude, as well as by parameters of the loop: the radius, the temperature (which prescribes the sound speed and local scale height) and the dissipation coefficient. For the propagating disturbances observed in the coronal loops, some of the parameters are determined: the wave periods are 300–900 s, the relative amplitudes are about 2%, the loop radii are about 140 Mm, the temperature is 1.6 MK. The most unknown parameter is the dissipation coefficient, because both viscosity and thermal conduction have not been determined observationally yet. According to Braginskii's theory, the first viscosity coefficient for the plasma with the concentration 5×10^8 cm^{-3} and the temperature 1.6 MK is $\eta_0 = 0.352$ g(cm s)$^{-1}$. This parameter coincides with the parameter η used above, which, neglecting the thermal conduction ($\gamma = 1$), gives $\bar{\eta} \approx 4 \times 10^{-4}$. Consequently, this is the least possible value of $\bar{\eta}$. In the presence of finite thermal condition this value can be higher. Also, as it has been suggested by Nakariakov et al. (1999) for shear viscosity,

the actual MHD wave dissipation can be dramatically enhanced (by, e.g. micro-turbulence).

In Fig. 3, we show dependences of the slow wave amplitudes upon the distance along the loop for three different wave periods and two different dissipation coefficients. It is seen that the theory developed easily explains the observational fact the descending wave is not registered: its amplitude is much weaker than the amplitude of the ascending wave. Also, the ascending wave amplitude growth can be efficiently depressed by dissipative processes.

5. Conclusions

We present here a theoretical model for slow magnetoacoustic waves propagating along magnetic field lines in coronal loops. The model incorporates the effects of dissipation due to finite viscosity and thermal conduction, gravitational stratification and nonlinearity. It is shown that, in the short wave length limit, the evolution of the waves is described by evolutionary equation (27). This equation is of Burgers type, but with an additional "geometrical" term and with coefficients dependent of the evolutionary coordinate. Investigation of solutions of the evolutionary equation shows that the propagating compressive disturbances observed in coronal loops can be confidently interpreted as slow magnetoacoustic waves. This interpretation meets all observationally detected properties of the propagating disturbances.

The theory confirms that there can be longitudinally propagating slow magnetoacoustic waves, perturbing the density of the plasma in the loop. The speed of these waves is to be registered below (taking into account possible projection effects) the sound speed. The waves of observed periods (5–15 min) are strongly affected by the gravitational stratification and dissipation. For the estimated dissipation of the waves (for typical coronal loop conditions, dimensionless coefficient of dissipation (29) is greater than 4×10^{-4}), the typical scenario of the upwardly propagating wave evolution is the following: initially, the relative amplitude of the waves grows with height and reach a maximum somewhere near the loop apex, and then quickly dissipate. The fact that there are no downwardly propagating waves confirms this interpretation. Indeed, the waves of observed periods dissipate in the upper parts of the loops and in the descending stage, their amplitude is below the noise level. Waves of longer periods (10–15 min) are less affected by the dissipation, while the short period waves ($<$5 min) are practically evanescent, because the dissipation length becomes comparable with the wavelength. In addition, the effective dissipation of the short period waves in the loops can be responsible for the absence of the short time periodicities in intensity variations on an active region, reported by Ireland et al. (1999).

According to our findings, the nonlinearity does not play an important role in the dynamics and dissipation of the waves. Indeed, only waves with initial amplitudes higher than 8–10% can be significantly distorted by the nonlinear generation of higher harmonics. Waves of lower amplitudes (e.g. of observed 1–2% in density) keep their initial shape. This is supported by the observations: Fig. 11 of Berghmans & Clette (1999) and Fig. 2 of De Moortel et al. (2000) do not show any signs of the wave distortion.

De Moortel et al. (2000) have deduced that the observed energy of the waves is insufficient for heating of coronal loops. However, the waves can be used as a tool for MHD coronal seismology. Indeed, combining the observationally measured properties of the waves with theoretical models, we can determine additional parameters of the coronal plasma (cf. Nakariakov at al. 1999). For example, accurate measurement of the wave amplitude as a function of the vertical coordinate and comparing this with the theoretical dependences (see Fig. 4), we can estimate the dissipative coefficient $\bar{\eta}$, connected with the coronal viscosity and thermal conduction (29).

The application of the method of MHD coronal seismology requires not only precise observations, but also elaborated theory. The theoretical model developed in this study is quite a simple one and neglects several physical mechanisms which can be important for the slow wave evolution. One of these neglected mechanisms is reflection of the waves from the density gradient. The WKB method used in the derivation of the evolutionary equation does not allow us to take into account the reflection. So, the waves of longer wavelengths, comparable with the scale height, can experience the reflection. In principle, this effect has to be taken into account. However, we can probably neglect this effect, according to results of Ofman et al. (1999), which show that the reflection of slow magnetoacoustic waves from density gradients in polar plumes is insignificant and the WKB approach works very well in the plume case. Anyway, the detailed study of the effect should be done in the future. Another effect neglected is dispersion of slow magnetoacoustic modes of a loop, connected with the finite radius of the loop cross-section. For example, it is well known that fast modes of coronal loops are strongly dispersive in the long wavelength limit, and their phase and group speeds are strongly influenced by the dispersion (Roberts et al. 1983, 1984). In contrast, slow modes are very weakly dispersive and the dispersion becomes important only in the nonlinear regime. The dispersion can slow down the nonlinear generation of higher harmonics and is very important on the nonlinear stage of the wave evolution (see, e.g. Zhugzhda & Nakariakov 1997a,b for slow body sausage modes of coronal loops). But, as the nonlinearity is found to be insignificant for the amplitude observed, the neglect of this effect also seems to be justified. Also, more developed models have to include the gradient of the temperature along the loop (see Aschwanden et al. 1999b) and effects of variable loop cross-section.

Thus, we believe that the model developed provides the correct *qualitative* interpretation of running intensity disturbances in coronal loops as slow magnetoacoustic waves and can be used as a basis for seismology of the coronal loops.

Acknowledgements. VMN is grateful to Bernie Roberts and Leon Ofman for a number of insightful discussions, and to Tony Arber for the help with the numerical solution of the evolutionary equation. EV and DB acknowledge the support of the Belgian Federal Services of Scientific, Technical and Cultural Affairs (SSTC/DWTC). EV, DB and ER would like to thank Jean-Francois Hochedez for the many useful dis-

cussions. The authors are grateful to the referee, Markus Aschwanden, for help with the paper improvement.

References

Antonucci E., Gabriel A.H., Patchett B.E., 1984, Solar Phys. 93, 85
Aschwanden M.J., 1987, Solar Phys. 111, 113
Aschwanden M.J., Fletcher L., Schrijver C.J., Alexander D., 1999a, ApJ 520, 880
Aschwanden M.J., Newmark J.S., Delaboudiniere J.-P., et al., 1999b, ApJ 515, 842
Berghmans D., Clette F., 1999, Solar Phys. 186, 207
Berghmans D., Clette F., Robbrecht E., McKenzie D., 1999, ESA SP-448, 575
Chapman R.D., Jordan S.D., Neupert W.M., Thomas R.J., 1972, ApJ 174, L97
Deforest C.E., Gurman J.B., 1998, ApJ 501, L217
De Moortel I., Ireland J., Walsh R.W., 2000, A&A 355, L23-L26
Harrison R.A., 1987, A&A 182, 337
Ireland J., Walsh R.W., Harrison R.A., Priest E.R., 1999, A&A 347, 355
Koutchmy S., Zugzda Y.D., Locans V., 1983, A&A 10, 185
Nakariakov V.M., Ofman L., DeLuca E.E., Roberts B., Davila J.M., 1999, Sci 285, 862
Ofman L., Nakariakov V.M., Deforest C.E., 1999, ApJ 514, 441
Ofman L., Nakariakov V.M., Sehgal N., 2000, ApJ 533, 1071
Ofman L., Romoli M., Poletto G., Noci G., Kohl J.L., 1997, ApJ 491, L111
Ofman L., Romoli M., Poletto G., Noci G., Kohl J.L., 1998, ApJ 507, L189
Ofman L., Romoli M., Poletto G., Noci G., Kohl J.L., 2000, ApJ 529, 592
Oliver R., 1999, ESA SP-448, 575
Robbrecht E., Berghmans D., Poedts, S., 1999, ESA SP-446, 575
Robbrecht E., Verwichte E., Berghmans D., et al., 2000, A&A submitted
Roberts B., Edwin P.M., Benz A.O., 1983, Nat 305, 688
Roberts B., Edwin P.M., Benz A.O., 1984, ApJ 279, 857
Thompson B.J., Gurman J.B., Neupert W.M., et al., 1999, ApJ 517, L151
Zhugzhda Y.D., Nakariakov V.M., 1997a, Phys. Let. A 233, 413
Zhugzhda Y.D., Nakariakov V.M., 1997b, Solar Phys. 175, 107